

Magnetization and magnetic phase diagrams of a spin-1/2 ferrimagnetic diamond chain at low temperature

Tai-Min Cheng(成泰民), Mei-Lin Li(李美霖), Zhi-Rui Cheng(成智睿), Guo-Liang Yu(禹国梁)[1], Shu-Sheng Sun(孙树生)[1], Chong-Yuan Ge(葛崇员)[1], Xin-Xin Zhang(张新欣)[1]

Citation: Chin. Phys. B, 2021, 30 (**5**): 057503. DOI: 10.1088/1674-1056/abd768
Journal homepage: http://cpb.iphy.ac.cn; http://iopscience.iop.org/cpb

What follows is a list of articles you may be interested in

Field-induced N\'eel vector bi-reorientation of a ferrimagnetic insulator in the vicinity of compensation temperature

Peng Wang(王鹏), Hui Zhao(赵辉), Zhongzhi Luan(栾仲智), Siyu Xia(夏思宇), Tao Feng(丰韬), and Lifan Zhou(周礼繁)
Chin. Phys. B, 2021, 30 (**2**): 027501. DOI: 10.1088/1674-1056/abbbef

Computational study of inverse ferrite spinels

A EL Maazouzi, R Masrour, A Jabar, M Hamedoun
Chin. Phys. B, 2019, 28 (**5**): 057504. DOI: 10.1088/1674-1056/28/5/057504

Dyson-Maleev theory of an *X X Z* ferrimagnetic spin chain with single-ion anisotropy

Yu-Ge Chen(陈宇戈), Yin-Xiang Li(李殷翔), Li-Jun Tian(田立君), Bin Chen(陈斌)
Chin. Phys. B, 2018, 27 (**12**): 127501. DOI: 10.1088/1674-1056/27/12/127501

Magnetism induced by Mn atom doping in SnO monolayer

Ruilin Han(韩瑞林), Yu Yan(闫羽)
Chin. Phys. B, 2018, 27 (**11**): 117505. DOI: 10.1088/1674-1056/27/11/117505

Ferromagnetism and magnetostructural coupling in V-doped MnNiGe alloys

Hui Yang(杨慧), Jun Liu(刘俊), Chao Li(李超), Guang-Long Wang(王广龙), Yuan-Yuan Gong(龚元元), Feng Xu(徐锋)
Chin. Phys. B, 2018, 27 (**10**): 107502. DOI: 10.1088/1674-1056/27/10/107502

Magnetization and magnetic phase diagrams of a spin-1/2 ferrimagnetic diamond chain at low temperature*

Tai-Min Cheng(成泰民)[1,2,†], Mei-Lin Li(李美霖)[1,2], Zhi-Rui Cheng(成智睿)[3], Guo-Liang Yu(禹国梁)[1], Shu-Sheng Sun(孙树生)[1], Chong-Yuan Ge(葛崇员)[1], and Xin-Xin Zhang(张新欣)[1]

[1] *Department of Physics, College of Sciences, Shenyang University of Chemical Technology, Shenyang* 110142, *China*
[2] *School of Materials Science and Engineering, Shenyang University of Chemical Technology, Shenyang* 110142, *China*
[3] *School of Software Engineering, Shenyang University of Technology, Shenyang* 110870, *China*

(Received 4 November 2020; revised manuscript received 21 December 2020; accepted manuscript online 30 December 2020)

We used the Jordan–Wigner transform and the invariant eigenoperator method to study the magnetic phase diagram and the magnetization curve of the spin-1/2 alternating ferrimagnetic diamond chain in an external magnetic field at finite temperature. The magnetization versus external magnetic field curve exhibits a 1/3 magnetization plateau at absolute zero and finite temperatures, and the width of the 1/3 magnetization plateau was modulated by tuning the temperature and the exchange interactions. Three critical magnetic field intensities $H_{\rm CB}$, $H_{\rm CE}$ and $H_{\rm CS}$ were obtained, in which the $H_{\rm CB}$ and $H_{\rm CE}$ correspond to the appearance and disappearance of the 1/3 magnetization plateau, respectively, and the higher $H_{\rm CS}$ correspond to the appearance of fully polarized magnetization plateau of the system. The energies of elementary excitation $\hbar\omega_{\sigma,k}$ ($\sigma = 1,2,3$) present the extrema of zero at the three critical magnetic fields at 0 K, i.e., $\left[\hbar\omega_{3,k}(H_{\rm CB})\right]_{\rm min} = 0$, $\left[\hbar\omega_{2,k}(H_{\rm CE})\right]_{\rm max} = 0$ and $\left[\hbar\omega_{2,k}(H_{\rm CS})\right]_{\rm min} = 0$, and the magnetic phase diagram of magnetic field versus different exchange interactions at 0 K was established by the above relationships. According to the relationships between the system's magnetization curve at finite temperatures and the critical magnetic field intensities, the magnetic field-temperature phase diagram was drawn. It was observed that if the magnetic phase diagram shows a three-phase critical point, which is intersected by the ferrimagnetic phase, the ferrimagnetic plateau phase, and the Luttinger liquid phase, the disappearance of the 1/3 magnetization plateau would inevitably occur. However, the 1/3 magnetization plateau would not disappear without the three-phase critical point. The appearance of the 1/3 magnetization plateau in the low temperature region is the macroscopic manifestations of quantum effect.

Keywords: invariant eigen-operator method, Jordan–Wigner transformations, critical magnetic field intensity, magnetic phase diagrams

PACS: 75.50.Gg, 68.65.−k, 75.30.Kz **DOI:** 10.1088/1674-1056/abd768

1. Introduction

Low-dimensional frustration quantum magnetic systems have attracted much attention since they exhibit strange quantum phenomena, which are closely related to the low-temperature quantum phase transition of low-dimensional condensed matter.[1–8] Especially in the diamond-chain compound $Cu_3(CO_3)_2(OH)_2$ single crystal,[2] the 1/3 magnetization plateau and double peaks of magnetic susceptibility and specific heat were observed experimentally. This triggered intensive research interests in such low-dimensional magnetic chain materials.[3–7] Rule *et al.*[5] used inelastic neutron scattering experiments to investigate the exchange integrals of the diamond chain compound azurite $Cu_3(CO_3)_2(OH)_2$ and again confirmed the existence of the 1/3 magnetization plateau from the experiment. Jeschke *et al.*[6] theoretically investigated the magnetic properties and the exchange integrals of the spin-1/2 diamond chain with density functional theory and explained the formation mechanism of the frustrated material with first-principles. In the calculation of properties in low-dimensional magnetic quantum systems, the density-matrix renormalization group[9] (DMRG) method exhibits its advantages. For example, the DMRG method is employed in the phase diagram[3,4] study of the one-dimensional magnetic quantum chain system.

In addition, there are also other theoretical methods to study the magnetic and thermodynamic properties of one-dimensional magnetic chain, e.g., the transfer-matrix density-matrix renormalization group method[7,8] (TMRG), the invariant eigen-operator (IEO) method[10–12] combined with Jordan–Wigner (J–W) transformations,[13,14] and the spin-wave theory[15] method from a fully polarized vacuum combined with the quantum Monte Carlo (QMC) simulation.[15] The magnetic-field vs temperature phase diagram of alternate ferrimagnetic chains reported in the paper of Silva and Montenegro-Filho[15] has caught our attention. In their work, the relationship between the critical magnetic field and the double peak of magnetic susceptibility, as well as the correlation between the magnetization curve and the magnetic phase

*Project supported by the National Natural Science Foundation of China (Grant Nos. 11374215 and 11704262), the Scientific Study Project from Education Department of Liaoning Province of China (Grant No. LJ2019004), and the Natural Science Foundation Guidance Project of Liaoning Province of China (Grant No. 2019-ZD-0070).

†Corresponding author. E-mail: ctm701212@126.com; chengtaimin@syuct.edu.cn

© 2021 Chinese Physical Society and IOP Publishing Ltd

diagram, have attracted our great interest.

We have specifically investigated the properties of a spin-1/2 ferrimagnetic diamond XY chain[10] with the IEO method, two peaks in magnetic susceptibility and specific heat as well as two valleys in entropy appear at the critical magnetic field, which are similar to Silva's work,[15] and the two peaks are also very similar in height. This triggered our motivation to investigate the magnetic phase diagram of the one-dimensional magnetic chain system with the IEO method.

The elementary excitation of the spin-1/2 ferrimagnetic chain system is also a fermion-type collective excitation that satisfies the Pauli exclusion principle. This fermion-type collective excitation is closely related to the Luttinger liquid (LL) phase in one-dimensional quantum wires. The quantum critical point separates a gapped insulating phase and a gapless conducting phase. The quantum critical state can be experimentally accessed through an applied magnetic field in magnetic insulators.[16,17] In these systems, the gapped phases are associated with magnetization plateaus in the magnetization curves. Oshikawa *et al.*[18] clarified that this magnetization plateau should be understood as a topological effect.

In this paper, the alternating ferrimagnetic diamond chain of the one-dimensional spin-1/2 Heisenberg with long-range interaction in the external magnetic field was investigated using the IEO method[10–12] combined with J–W transformations. Therefore, we derived the elementary-excitation energy spectra and partition function of the system under the external magnetic field. We only conducted a detailed study of the magnetization and the magnetic phase diagram of the system at absolute zero and finite temperature. Given the partition function of the system under the external magnetic field, it is easy to obtain the expressions of additional thermodynamic and magnetic physical quantities of the system (such as specific heat, internal energy, free energy, entropy, magnetic susceptibility).

2. The partition function and elementary excitations of the system

As shown in Fig. 1, dimer and monomer are alternately arranged to form a ferrimagnetic diamond chain with 1/2 spin. Here S_{l,d_1} and S_{l,d_2} represent the dimer's spin quantum, and $S_{l,m}$ represents the monomer's spin quantum. Suppose that such a system has an N ($l = 1,2,\ldots,N$) cyclic structure. We use the Heisenberg interaction theory model to describe, and the Hamiltonian of the system can be expressed as follows:

$$\begin{aligned}\hat{H} = \sum_{l=1}^{N}\Big\{ & J_2\hat{\boldsymbol{S}}_{l,d_1}\cdot\hat{\boldsymbol{S}}_{l,d_2} + J_1\hat{\boldsymbol{S}}_{l,m}\cdot\hat{\boldsymbol{S}}_{l,d_1} + J_3\hat{\boldsymbol{S}}_{l,m}\cdot\hat{\boldsymbol{S}}_{l,d_2} \\ & + \frac{J_1}{2}\left[\hat{\boldsymbol{S}}_{l,d_2}\cdot\hat{\boldsymbol{S}}_{l-1,m} + \hat{\boldsymbol{S}}_{l+1,d_2}\cdot\hat{\boldsymbol{S}}_{l,m}\right] \\ & + \frac{J_3}{2}\left[\hat{\boldsymbol{S}}_{l,d_1}\cdot\hat{\boldsymbol{S}}_{l-1,m} + \hat{\boldsymbol{S}}_{l+1,d_1}\cdot\hat{\boldsymbol{S}}_{l,m}\right] \\ & + \frac{J_m}{2}\left[\hat{\boldsymbol{S}}_{l-1,m}\cdot\hat{\boldsymbol{S}}_{l,m} + \hat{\boldsymbol{S}}_{l,m}\cdot\hat{\boldsymbol{S}}_{l+1,m}\right] \\ & + g u_{\mathrm{B}} H\left(\hat{S}^z_{l,d_1} + \hat{S}^z_{l,d_2} + \hat{S}^z_{l,m}\right)\Big\}. \end{aligned} \tag{1}$$

In Eq. (1) $\hat{\boldsymbol{S}}_{l,d_1}$, $\hat{\boldsymbol{S}}_{l,d_2}$ and $\hat{\boldsymbol{S}}_{l,m}$ are spin quantum operators of spin 1/2, $\hat{\boldsymbol{S}}_{l,d_1}$ and $\hat{\boldsymbol{S}}_{l,d_2}$ are coupled by the ferromagnetic interaction J_2 ($J_2 < 0$) in dimer molecule, $\hat{\boldsymbol{S}}_{l,m}$ and $\hat{\boldsymbol{S}}_{l+1,m}$ are coupled by the ferromagnetic interactions J_m ($J_m < 0$) between monomer and monomer molecules, $\hat{\boldsymbol{S}}_{l,d_1}$ and $\hat{\boldsymbol{S}}_{l+1,m}$ are coupled by the anti-ferromagnetic interaction between dimers and monomer molecules J_1 ($J_1 > 0$), $\hat{\boldsymbol{S}}_{l,d_2}$ and $\hat{\boldsymbol{S}}_{l+1,m}$ are coupled by anti-ferromagnetic interaction between dimers and monomer molecules J_3 ($J_3 > 0$), $\hat{\boldsymbol{S}}_{l,d_2}$ and $\hat{\boldsymbol{S}}_{l,m}$ are coupled by the anti-ferromagnetic interaction between dimers and monomer molecules J_1, $\hat{\boldsymbol{S}}_{l,d_1}$ and $\hat{\boldsymbol{S}}_{l,m}$ are coupled by the anti-ferromagnetic interaction between dimers and monomer molecules J_3. u_{B} is the Bohr magneton, g is the Landé factor, and H is the intensity of the external magnetic field.

We apply J–W transformation[13,14] to the spin operators in Eq. (1)

$$\begin{aligned} S^+_{l,m} &= a_l^+ \exp\left[\mathrm{i}\pi\sum_{i=1}^{l-1}\left(a_i^+a_i + b_i^+b_i + c_i^+c_i\right)\right], \\ S^+_{l,d_1} &= b_l^+ \exp\left[\mathrm{i}\pi\sum_{i=1}^{l}\left(a_i^+a_i\right) + \mathrm{i}\pi\sum_{i=1}^{l-1}\left(b_i^+a_i + c_i^+c_i\right)\right], \\ S^+_{l,d_2} &= c_l^+ \exp\left[\mathrm{i}\pi\sum_{i=1}^{l}\left(a_i^+a_i + b_i^+b_i\right) + \mathrm{i}\pi\sum_{r=1}^{l-1}\left(c_i^+c_i\right)\right], \\ S^z_{l,m} &= a_l^+a_l - \frac{1}{2},\ S^z_{l,d_1} = b_l^+b_l - \frac{1}{2},\ S^z_{l,d_2} = c_l^+c_l - \frac{1}{2}, \end{aligned} \tag{2}$$

where operators a_i, b_i and c_i are Fermion operators, they satisfy the anti-commutation relations $[a_i, a_j^+]_+ = \delta_{i,j}$, $[b_i, b_j^+]_+ = \delta_{i,j}$ and $[c_i, c_j^+]_+ = \delta_{i,j}$.

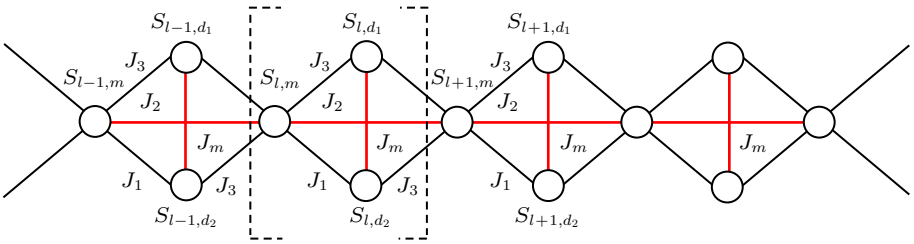


Fig. 1. The alternating ferrimagnetic diamond chain of the one-dimensional spin-1/2 Heisenberg model is composed of dimers and monomers.

The lattice Fourier transforms for operators a_l, b_l and c_l are as follows:

$$\begin{aligned} a_l &= N^{-1/2}\sum_k \exp(\mathrm{i}kl)\, a_k, \\ b_l &= N^{-1/2}\sum_k \exp(\mathrm{i}kl)\, b_k, \\ c_l &= N^{-1/2}\sum_k \exp(\mathrm{i}kl)\, c_k. \end{aligned} \tag{3}$$

In Eq. (3), a_k (a_k^+), b_k (b_k^+) and c_k (c_k^+) also satisfy the anti-commutation relations, and N is the number of primitive cells in the system.

According to Eqs. (1)–(3), and $N^{-1}\sum\limits_{l=1}^{N}\exp[\mathrm{i}(k'-k)l] = \delta_{k',k}$, the system Hamiltonian under linear approximation can be obtained

$$\hat{H} = \sum_k \hat{H}_k - \frac{3gu_{\mathrm{B}}HN}{2} + \frac{N}{4}(J_m + 2J_1 + J_2 + 2J_3), \tag{4}$$

where

$$\begin{aligned} \hat{H}_k = \frac{1}{2}\{&[(J_1+\gamma_k^* J_3)a_k^+ b_k + (J_3+\gamma_k^* J_1)a_k^+ c_k + J_2 b_k^+ c_k] + \mathrm{h.c.} \\ &+ h_1 a_k^+ a_k + h_2 b_k^+ b_k + h_2 c_k^+ c_k\}, \end{aligned} \tag{5}$$

in which $\gamma_k = \mathrm{e}^{\mathrm{i}ka}$, where a is the periodic lattice constant of the system,

$$\begin{aligned} h_1 &= 2gu_{\mathrm{B}}H + 2J_m(\cos ka - 1) - 2J_1 - 2J_3, \\ h_2 &= 2gu_{\mathrm{B}}H - J_1 - J_2 - J_3. \end{aligned} \tag{6}$$

According to Eqs. (5) and (6) and the anti-commutation relations of operators, we can obtain

$$\begin{aligned} [a_k, \hat{H}]_- &= [a_k, \hat{H}_k]_- \\ &= \frac{1}{2}[h_1 a_k + (J_1 + \gamma_k^* J_3) b_k + (J_3 + \gamma_k^* J_1) c_k], \\ [b_k, \hat{H}]_- &= [b_k, \hat{H}_k]_- \\ &= \frac{1}{2}[(J_1 + \gamma_k J_3) a_k + h_2 b_k + J_2 c_k], \\ [c_k, \hat{H}]_- &= [c_k, \hat{H}_k]_- \\ &= \frac{1}{2}[(J_2 + \gamma_k J_1) a_k + J_2 b_k + h_2 c_k]. \end{aligned} \tag{7}$$

For a systemic Hamiltonian $\hat{H}$, the IEO[11,12] of operators a_k, b_k and c_k are operators $\hat{O}_{e,\sigma}$ ($\sigma = 1,2,3$), where

$$(\hat{O}_{e,1}\ \hat{O}_{e,2}\ \hat{O}_{e,3}) = (a_k\ b_k\ c_k)U. \tag{8}$$

In Eq. (8)

$$U = \begin{pmatrix} \tau_{11} & \tau_{12} & \tau_{13} \\ \tau_{21} & \tau_{22} & \tau_{23} \\ \tau_{31} & \tau_{32} & \tau_{33} \end{pmatrix}. \tag{9}$$

Equation (8) can be described as

$$\begin{aligned} \hat{O}_{e,\sigma} &= \tau_{1,\sigma} a_k + \tau_{2,\sigma} b_k + \tau_{3,\sigma} c_k \\ &= (a_k\ b_k\ c_k)\begin{pmatrix} \tau_{1,\sigma} \\ \tau_{2,\sigma} \\ \tau_{3,\sigma} \end{pmatrix}, \quad (\sigma = 1,2,3), \end{aligned} \tag{10}$$

$$[\hat{O}_{e,\sigma}, \hat{H}]_- = [\hat{O}_{e,\sigma}, \hat{H}_k]_- = \lambda_\sigma \hat{O}_{e,\sigma}, \quad (\sigma = 1,2,3), \tag{11}$$

where $\tau_{1,\sigma}$, $\tau_{2,\sigma}$ and $\tau_{3,\sigma}$ are complex numbers.

From Eqs. (4)–(11), we can derive the equation as follows:

$$\begin{aligned} &\begin{pmatrix} h_1/2 & (J_1 + J_3\gamma_k)/2 & (J_3 + J_1\gamma_k)/2 \\ (J_1 + J_3\gamma_k^*)/2 & h_2/2 & J_2/2 \\ (J_3 + J_1\gamma_k^*)/2 & J_2/2 & h_2/2 \end{pmatrix}\begin{pmatrix} \tau_{1,\sigma} \\ \tau_{2,\sigma} \\ \tau_{3,\sigma} \end{pmatrix} \\ &= \lambda_\sigma \begin{pmatrix} \tau_{1,\sigma} \\ \tau_{2,\sigma} \\ \tau_{3,\sigma} \end{pmatrix}. \end{aligned} \tag{12}$$

From the secular equation[19,20] of Eq. (12), the energies of the elementary excitations of the system are obtained as follows:

$$\begin{aligned} \hbar\omega_{\sigma,k} = \lambda_\sigma = 2\sqrt{-p/3}\cos([u + (\sigma-1)2\pi/3]) - b/3, \\ (\sigma = 1,2,3), \end{aligned} \tag{13}$$

in which

$$\begin{aligned} u &= \arccos\left[(-\tau/2)(-p/3)^{-3/2}\right]/3, \quad p = c - b^2/3, \\ \tau &= d - bc/3 + 2b^3/27, \\ b &= -(h_1 + 2h_2)/2, \\ c &= \left\{2h_1h_2 + h_2h_2 - \left[2J_1^2 + J_2^2 + 2J_3^2 + 4J_1J_3\cos k\right]\right\}/4, \\ d &= \left[J_2^2 h_1 + 2\left(J_1^2 + J_3^2 + 2J_1J_3\cos k\right)h_2 - h_1h_2h_2\right]/8 \\ &\quad - J_2\left[2J_1J_3 + \left(J_1^2 + J_3^2\right)\cos k\right]/4. \end{aligned} \tag{14}$$

By the inverse transformation of Eq. (8) and using the unitarity of matrix U ($U^{-1} = U^+$), we obtain

$$\begin{aligned} (a_k\ b_k\ c_k) &= (\hat{O}_{e,1}\ \hat{O}_{e,2}\ \hat{O}_{e,3})U^{-1} = (\hat{O}_{e,1}\ \hat{O}_{e,2}\ \hat{O}_{e,3})U^+ \\ &= (\hat{O}_{e,1}\ \hat{O}_{e,2}\ \hat{O}_{e,3})\begin{pmatrix} \tau_{11}^* & \tau_{21}^* & \tau_{31}^* \\ \tau_{12}^* & \tau_{22}^* & \tau_{32}^* \\ \tau_{13}^* & \tau_{23}^* & \tau_{33}^* \end{pmatrix}. \end{aligned} \tag{15}$$

Take Hermite conjugate on both sides of Eq. (15)

$$\begin{pmatrix} a_k^+ \\ b_k^+ \\ c_k^+ \end{pmatrix} = \begin{pmatrix} \tau_{11} & \tau_{12} & \tau_{13} \\ \tau_{21} & \tau_{22} & \tau_{23} \\ \tau_{31} & \tau_{32} & \tau_{33} \end{pmatrix}\begin{pmatrix} \hat{O}_{e,1}^+ \\ \hat{O}_{e,2}^+ \\ \hat{O}_{e,3}^+ \end{pmatrix}. \tag{16}$$

According to the anti-commutation relations in the a_k (a_k^+), b_k (b_k^+) and c_k (c_k^+), easy access to $\hat{O}_{e,\sigma}(\hat{O}_{e,\sigma}^+)$ also has anti-commutation relations $[\hat{O}_{e,i}, \hat{O}_{e,j}^+]_+ = \delta_{ij}$ and $[\hat{O}_{e,i}, \hat{O}_{e,j}]_+ = [\hat{O}_{e,i}^+, \hat{O}_{e,j}^+]_+ = 0$. Therefore, there is $(\hat{O}_{e,\sigma}^+\hat{O}_{e,\sigma})^2 - \hat{O}_{e,\sigma}^+\hat{O}_{e,\sigma} = 0$ (which is $\hat{n}_{e,\sigma}(\hat{n}_{e,\sigma} - 1) = 0$), so the eigenvalue of the particle-number operators $\hat{n}_{e,\sigma}$ is 0 or 1. And the statistical average of particle-number operators $\hat{n}_{e,\sigma}$ satisfies the Fermi–Dirac statistical distribution $\langle\hat{n}_{e,\sigma}\rangle = \{\mathrm{e}^{\hbar\beta\omega_{\sigma,k}} + 1\}^{-1}$.

From Eqs. (4), (5), (11), (15), and (16), the diagonalization of the Hamiltonian of the system is derived as follows:

$$\begin{aligned} \hat{H} = &\sum_k \{\hbar\omega_{1,k}\hat{O}_{e1}^+\hat{O}_{e1} + \hbar\omega_{2,k}\hat{O}_{e2}^+\hat{O}_{e2} + \hbar\omega_{3,k}\hat{O}_{e3}^+\hat{O}_{e3}\} \\ &- \frac{3gu_{\mathrm{B}}HN}{2} + \frac{N}{4}(J_m + 2J_1 + J_2 + 2J_3). \end{aligned} \tag{17}$$

From Eqs. (4) and (17), the partition function of the system

can be easily obtained as follows:

$$\begin{aligned} Z &= \mathrm{Tr}\exp(-\beta\hat{H}) \\ &= \exp\left\{-\beta\left[-\frac{3gu_{\mathrm{B}}HN}{2}+\frac{N}{4}(J_m+2J_1+J_2+2J_3)\right]\right\} \\ &\quad\times\prod_k\prod_{\sigma=1}^{3}\left(1+\mathrm{e}^{-\beta\lambda_\sigma}\right), \end{aligned} \tag{18}$$

where $\beta=\frac{1}{k_{\mathrm{B}}T}$.

Form Eq. (18), the Helmholtz free energy of the system can be obtained and are given as

$$\begin{aligned} F &= -\beta^{-1}\ln Z=-\frac{3gu_{\mathrm{B}}HN}{2}+\frac{N}{4}(J_m+2J_1+J_2+2J_3) \\ &\quad-\beta^{-1}\sum_k\sum_{\sigma=1}^{3}\ln\left(1+\mathrm{e}^{-\beta\lambda_\sigma}\right). \end{aligned} \tag{19}$$

The magnetization of the system can be obtained from Eq. (19) as

$$\begin{aligned} M &= -\left(\frac{\partial F}{\partial H}\right)_T=\frac{3gu_{\mathrm{B}}N}{2}-gu_{\mathrm{B}}\sum_k\sum_{\sigma=1}^{3}\frac{1}{1+\mathrm{e}^{\beta\lambda_\sigma}}\left(\frac{\partial\lambda_\sigma}{\partial h}\right) \\ &= gu_{\mathrm{B}}N\left\{\frac{3}{2}-\frac{a}{2\pi}\sum_{\sigma=1}^{3}\int_{-\pi}^{\pi}\frac{\mathrm{d}k}{1+\mathrm{e}^{\beta\lambda_\sigma}}\left(\frac{\partial\lambda_\sigma}{\partial h}\right)\right\}, \\ &\qquad(\sigma=1,2,3), \end{aligned} \tag{20}$$

in which $h=gu_{\mathrm{B}}H$.

3. Analysis and discussion

From the temperature-dependent thermal disorder energy ($k_{\mathrm{B}}T$), the Zeeman energy ($gu_{\mathrm{B}}H$) that related to the external magnetic field, the ferromagnetic exchange energy (J_2) that makes the electron spins in the dimer molecule parallel to each other, the antiferromagnetic exchange energy (J_1 and J_3) that makes the electron spins between dimers and monomer molecules antiparallel arranged and the ferromagnetic exchange energy (J_m) which makes the electron spins of monomers and monomer molecules aligned in parallel, etc. Using the competition between the above energies, the magnetization behavior of the alternating ferrimagnetic diamond chain with a spin of 1/2 under an external magnetic field was analyzed.

To this end, when we change the exchange integral (J_1, J_2, J_3, J_m), we study the change of the system's magnetization with the external magnetic field at absolute zero and finite temperature. Thus, three critical magnetic field intensities H_{CB}, H_{CE} and H_{CS} are obtained. Here H_{CB} represents the critical magnetic field intensity, at which the system begins to exhibit a 1/3 magnetization plateau, H_{CE} represents the critical magnetic field intensity where the 1/3 magnetization plateau disappears, and H_{CS} represents the critical magnetic field intensity where the system begins to exhibit the fully polarized (FP) plateau.

According to Eqs. (13) and (14), the elementary-excitation spectra of the system satisfies the relationship of $\hbar\omega_{1,k}>\hbar\omega_{3,k}>\hbar\omega_{2,k}$ in the entire Brillouin zone (where $\hbar\omega_{1,k}>0$, but $\hbar\omega_{3,k}$ and $\hbar\omega_{2,k}$ can be positive or negative).

When $H\geq H_{\mathrm{CS}}$, the energies of three elementary excitations are greater than zero in the Brillouin zone, and they drive the system from low energy state to high energy state, leading to an energy gap (UP gap) and the fully polarized (FP) plateau phase. FP phase appears when H is higher than H_{CS}. In this area, the magnetic moment of dimer molecules and the single matrix molecule is fully parallel to the external magnetic field, which is similar to that of the ferromagnetic phase. The whole system is fully polarized. When $H_{\mathrm{CS}}>H>H_{\mathrm{CE}}$, the energy of $\hbar\omega_{2,k}$ can be positive or negative, resulting in a gapless state of the system and the Luttinger liquid (LL) phase. LL phase emerges when the magnetic field intensity H is in the range of $H_{\mathrm{CE}}<H<H_{\mathrm{CS}}$. In this area, the magnetic moment of the monomer's molecule will rotate along the direction of the external magnetic field when the elementary excitation energy increases, which will induce the magnetic moment of dimer's molecules to deviate from the external magnetic field randomly. The projection of the total magnetic moment along the direction of the external magnetic field will increase with the external magnetic field. When $H_{\mathrm{CE}}\geq H\geq H_{\mathrm{CB}}$, the energy of $\hbar\omega_{2,k}$ appears to be negative. It transforms the system from a high energy state to a low energy state, leading to an energy gap (DN gap) and the ferrimagnetic (FRI, 1/3 magnetization) plateau phase. FRI plateau phase appeared when the magnetic field intensity H is in the range of $H_{\mathrm{CE}}\geq H\geq H_{\mathrm{CB}}$. In this area, the magnetic moment of the dimer's molecules is parallel to the external magnetic field, whereas the magnetic moment of the monomer's molecule is along the opposite direction. The total magnetic moment of the ferrimagnetic system is the maximum and remains unchanged with the increase of the external magnetic field. When $H_{\mathrm{CB}}>H$, the energy of $\hbar\omega_{3,k}$ can be positive or negative, inducing a gapless state of the system and the ferrimagnetic (FRI) phase. FRI phase is a disordered ferrimagnetic-like phase in which the magnetic moments of the dimer's molecule are arranged approximately antiparallel to the magnetic moments of the monomer's molecule, but the size of the magnetic moment is different. Moreover, in this phase, the projection of the total magnetic moment along the direction of the external magnetic field will increase with the external magnetic field.

Combined with Eq. (20) and Fig. 2, it can be seen that at absolute zero temperature, when the energy of the elementary-excitation spectrum is greater than zero, the Fermi–Dirac statistical distribution $\langle n_\sigma\rangle=1/(1+\mathrm{e}^{\hbar\omega_{\sigma,k}/(k_{\mathrm{B}}T)})$, ($\sigma=1,2,3$) is zero. Due to $\hbar\omega_{1,k}>0$, so $\langle n_1\rangle=0$. Moreover, the energy of the elementary-excitation spectra will increase with the increase of the external magnetic field intensity (see Fig. 2).

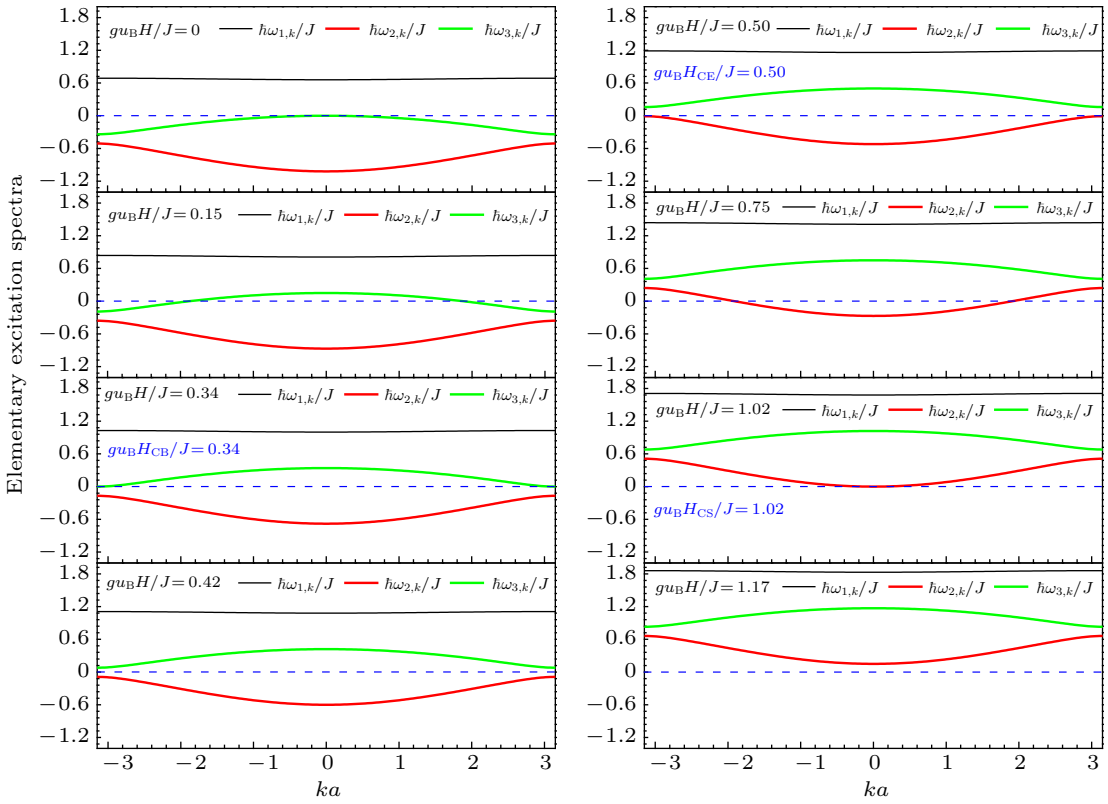


Fig. 2. The dispersion curves of elementary-excitation spectrum at 0 K in different external magnetic fields ($g\mu_B H/J = 0.0$, 0.15, 0.34, 0.42, 0.50, 0.75, 1.02, 1.17) (other parameters are set as $J_1/J = 0.47$, $J_2/J = -1$, $J_3/J = 0.21$, $J_m/J = -0.1$).

(i) When $\frac{g\mu_B H}{J} = 0$, in the entire Brillouin zone, the results of $\hbar\omega_{2,k} < 0$ (the red lines in Fig. 2) and $\hbar\omega_{3,k} < 0$ (the green lines in Fig. 2) with the corresponding Fermi–Dirac statistical distribution $\langle n_2\rangle = 1$ and $\langle n_3\rangle = 1$ can be obtained, which also results in $\frac{M}{g\mu_B N} = -0.5$. (ii) When $\frac{g\mu_B H}{J} = 0.34$, it is found that $(\hbar\omega_{3,k})_{\min} = 0$. Therefore, $\hbar\omega_{3,k} \geq 0$, in the whole Brillouin zone and induced $\langle n_3\rangle = 0$. However, if $\hbar\omega_{2,k} < 0$ in the whole Brillouin zone, the corresponding Fermi–Dirac statistical distribution will be $\langle n_2\rangle = 1$. Considering the above reasons, it can be obtained the results of $\frac{M}{g\mu_B N} = 0.5$, which is the critical magnetic field strength of H_{CB} where the 1/3 magnetization plateau appears. (iii) When $\frac{g\mu_B H}{J} = 0.5$, we can found $\hbar\omega_{3,k} > 0$, and thus $\langle n_3\rangle = 0$. However, when $(\hbar\omega_{2,k})_{\max} = 0$, $\hbar\omega_{2,k} \leq 0$ in the whole Brillouin zone. The corresponding Fermi–Dirac statistical distribution is $\langle n_2\rangle = 1$ and $\frac{M}{g\mu_B N} = 0.5$. Combined with the condition of $\frac{g\mu_B H}{J} = 0.75$, it can be known that $\hbar\omega_{2,k}$, which will be larger than zero at the boundary of the Brillouin zone and less than zero near the Γ point, leading to the system $1.5 > \frac{M}{g\mu_B N} > 0.5$. Considering the above, this corresponds to the critical magnetic field intensity H_{CE} corresponding to the disappearance of 1/3 of the magnetization plateau in the system. (iv) When $\frac{g\mu_B H}{J} = 1.02$, we can found $(\hbar\omega_{2,k})_{\min} = 0$. As a result, $\hbar\omega_{2,k} \geq 0$ holds for the whole Brillouin zone, which will induce $\langle n_2\rangle = 0$ and $\frac{M}{g\mu_B N} = 1.5$, which is the critical magnetic field intensity of H_{CS} where the saturated magnetization plateau appears.

The elementary excitations ($\hbar\omega_{1,k}$, $\hbar\omega_{2,k}$ and $\hbar\omega_{3,k}$) satisfy the Fermi–Dirac statistical distribution. The analysis of elementary-excitation spectra gives the relationship with the critical magnetic field as follows. Here H_{CB}, H_{CE}, and H_{CS} are the external magnetic field intensities as the minimum value of $\hbar\omega_{3,k}$, the maximum value of $\hbar\omega_{2,k}$, and the minimum value of $\hbar\omega_{2,k}$ are equal to zero, respectively. This can be expressed by the following equations:

$$\begin{aligned}
&[\hbar\omega_{3,k}(H_{CB})]_{\min} = 0,\\
&[\hbar\omega_{2,k}(H_{CE})]_{\max} = 0,\\
&[\hbar\omega_{2,k}(H_{CS})]_{\min} = 0.
\end{aligned} \tag{21}$$

We use Eq. (21) to draw the magnetic phase diagrams of magnetic field-different exchange integrals at absolute zero. The relationships between the system's magnetization curve at finite temperature and the critical external magnetic field intensities are obtained according to Eq. (20), and the magnetic field-temperature phase diagram is drawn.

In the magnetic phase diagrams, the FP plateau phase is represented in olive green, the LL phase is in blue, the FRI plateau phase (i.e., 1/3 magnetization plateau phase) is in magenta, and the FRI phase is in cyan (see Figs. 4, 6, 9 and 12).

It can be seen from Figs. 3 and 4 that in the spin-1/2 alternating ferrimagnetic diamond chain, when the reduced exchange integrals are $J_1/J = 0.47$, $J_2/J = -1$, $J_3/J = 0.21$, $J_m/J = -0.1$, the spin magnetic order of the system is destroyed by the thermal disorder energy with the increase of temperature. Therefore, the symmetry of the system increases,

and the order decreases. Its manifestation is in the low temperature range of $k_BT/J < 0.008$, the width of the 1/3 magnetization plateau of the system gradually decreases with the increase of temperature (see Figs. 3 and 4). The width of the 1/3 magnetization plateau is the largest at 0 K. As the temperature increases, the critical magnetic field intensity H_{CB} gradually increases (i.e., moves to the right), while the critical magnetic field intensity H_{CE} decreases (i.e., moves to the left), resulting in the width of 1/3 magnetization plateau gradually decreasing (see Fig. 3). Until $k_BT/J = 0.008$, the 1/3 magnetization plateau completely disappears. But the region of the spin-flop states (i.e., LL phase) gradually increases with increasing temperature. When $k_BT/J > 0.008$, the critical magnetic field intensity H_{CB} and H_{CE} of the system are completely coincident and are independent of temperature. The above analysis shows that the appearance of the 1/3 magnetization plateau of the system is closely related to the quantum effect of the system. Because the quantum effect of the system is more pronounced at extremely low temperatures, but this quantum effect is not observed at room temperature. This is because the quantum effects are completely suppressed by the thermal disorder energy at room temperature. Therefore, the appearance of the 1/3 magnetization plateau in the low temperature region is the macroscopic manifestation of the quantum effect. The critical temperature at which the 1/3 magnetization plateau disappears is $k_BT/J = 0.008$, this temperature corresponds to the three-phase critical point of the FRI phase, the FRI plateau phase, and the LL phase (see Fig. 4).

As can be seen from Figs. 5–7, when the reduced exchange integrals ($J_1/J = 0.47$, $J_3/J = 0.21$, $J_m/J = -0.14$), with the increase of reduced ferromagnetic exchange integral

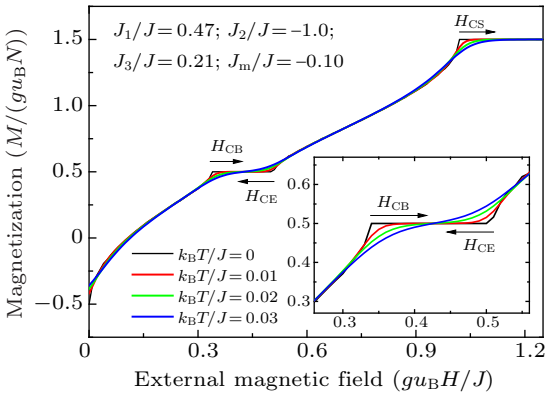


Fig. 3. The magnetization change with the external magnetic field at different temperatures (other parameters are set as $J_1/J = 0.47$, $J_2/J = -1$, $J_3/J = 0.21$, $J_m/J = -0.1$).

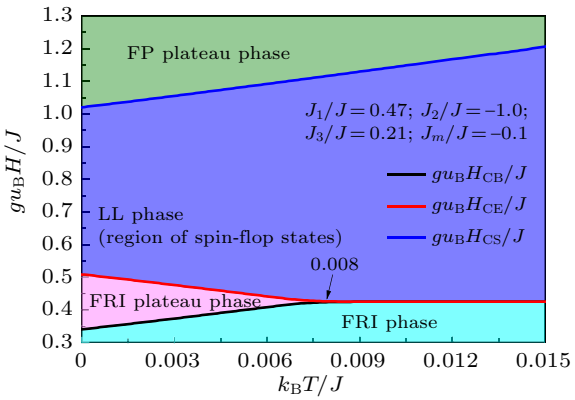


Fig. 4. The critical magnetic field intensities (H_{CB}, H_{CE} and H_{CS}) as a function of temperature (other parameters are set as $J_1/J = 0.47$, $J_2/J = 1.0$, $J_3/J = 0.21$, $J_m/J = -0.1$).

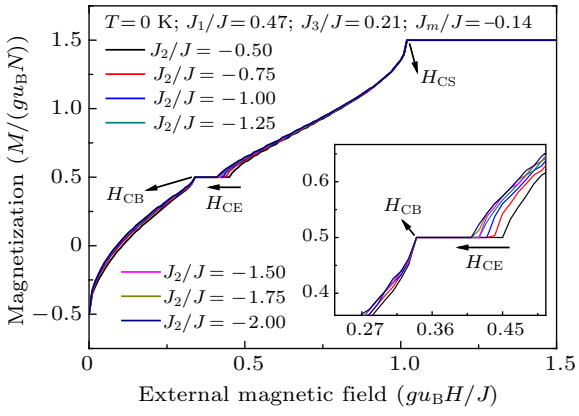


Fig. 5. The magnetization changes with the external magnetic field at $T = 0$ K, under different ferromagnetic exchange integrals J_2/J (-0.5, -0.75, -1.0, -1.25, -1.5, -1.75, -2.0) (other parameters are set as $J_1/J = 0.47$, $J_3/J = 0.21$, $J_m/J = -0.14$).

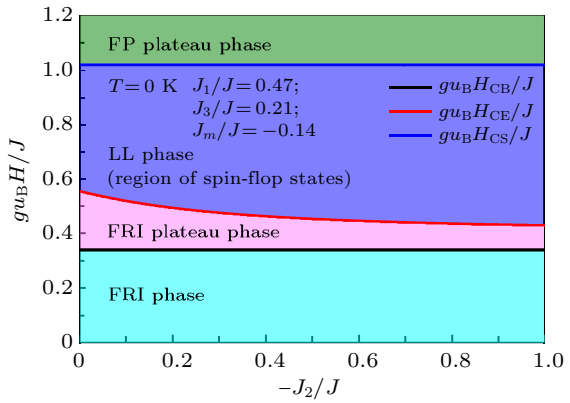


Fig. 6. The critical magnetic field intensities (H_{CB}, H_{CE} and H_{CS}) as a function of $-J_2/J$ at $T = 0$ K (other parameters are set as $J_1/J = 0.47$, $J_3/J = 0.21$, $J_m/J = -0.14$).

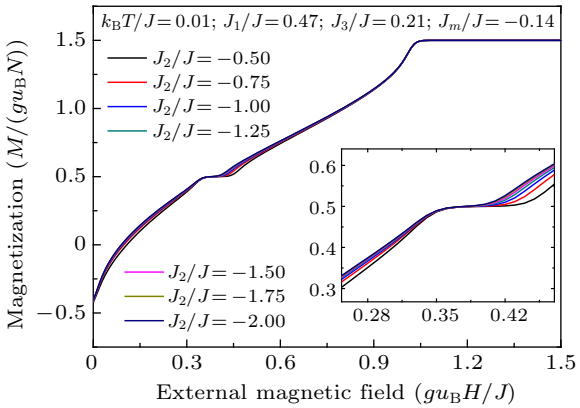


Fig. 7. The magnetization changes with the external magnetic field at finite temperature $k_BT/J = 0.01$, under different ferromagnetic exchange integrals J_2/J (-0.5, -0.75, -1.0, -1.25, -1.5, -1.75, -2.0) (other parameters are set as $J_1/J = 0.47$, $J_3/J = 0.21$, $J_m/J = -0.14$).

$-J_2/J$ (0.5, 0.75, 1.0, 1.25, 1.5, 1.75, 2.0), the critical magnetic field intensity H_{CE} decreases (i.e., moves to the left) at $T = 0$ K and finite temperature. However, the critical magnetic field intensities H_{CB} and H_{CS} do not change, which means that H_{CB} and H_{CS} have nothing to do with the ferromagnetic exchange energy (J_2) that makes the electron spins of the dimer molecules parallel. Therefore, as the reduced ferromagnetic exchange integral $-J_2/J$ increases, the region of the spin-flop states expands, and the width of the 1/3 magnetization plateau gradually decreases, but the decreasing rate becomes slower and slower and consequently, leading to the width of the 1/3 magnetization plateau tend to be constant. The thermal disorder energy k_BT destroys the magnetic order of the system (see Fig. 7), with the increase of the reduced ferromagnetic exchange integral $-J_2/J$, which accelerates the expansion of the region of spin-flop states and decreases the width of the 1/3 magnetization plateau. There is no three-phase critical point in the magnetic phase diagram, so the change of ferromagnetic exchange integral $-J_2/J$ does not cause the disappearance of 1/3 magnetization plateau (see Fig. 6).

In Fig. 8, when the reduced exchange integrals are $J_2/J = -1$, $J_3/J = 0.21$, $J_m/J = -0.14$, and the external magnetic field $gu_BH/J = 0$, and the reduced antiferromagnetic exchange integral $J_1/J = 0$, we can be obtained from Eqs. (13) and (14) that there are $\hbar\omega_{1,k} > 0$, $\hbar\omega_{3,k} > 0$, and $\hbar\omega_{2k} < 0$ in the entire Brillouin zone. And elementary excitations $\hbar\omega_{1,k}$, $\hbar\omega_{2,k}$ and $\hbar\omega_{3,k}$ satisfy the Fermi–Dirac statistical distribution. Therefore, from Eq. (20), it can be seen that when the external magnetic field $gu_BH/J = 0$, and $J_1/J = 0$, the total magnetization $M/(gu_BN) = 0.5$ at $T = 0$ K (see Fig. 8(a)). According to the principle of symmetry, the same result at 0 K should be obtained when $J_2/J = -1$, $J_1/J = 0.21$, $J_m/J = -0.14$, $gu_BH/J = 0$ and $J_3/J = 0$. However, as can be seen from Fig. 10(a), when the reduced exchange integrals are $J_2/J = -1.0$, $J_1/J = 0.47$, $J_m/J = -0.14$, the external magnetic field $gu_BH/J = 0$, and the reduced antiferromagnetic exchange integral $J_3/J = 0$, we can obtain from Eqs. (13) and (14) that there are $\hbar\omega_{1,k} > 0$, $\hbar\omega_{3,k} < 0$ and $\hbar\omega_{2,k} < 0$ in the entire Brillouin zone. So, from Eq. (20), we can know that when the external magnetic field $gu_BH/J = 0$, and $J_3/J = 0$, the total magnetization $M/(gu_BN) = -0.5$ at $T = 0$ K. Similarly, when $J_2/J = -1.0$, $J_3/J = 0.47$, $J_m/J = -0.14$, $gu_BH/J = 0$ and $J_3/J = 0$, the same result should be obtained.

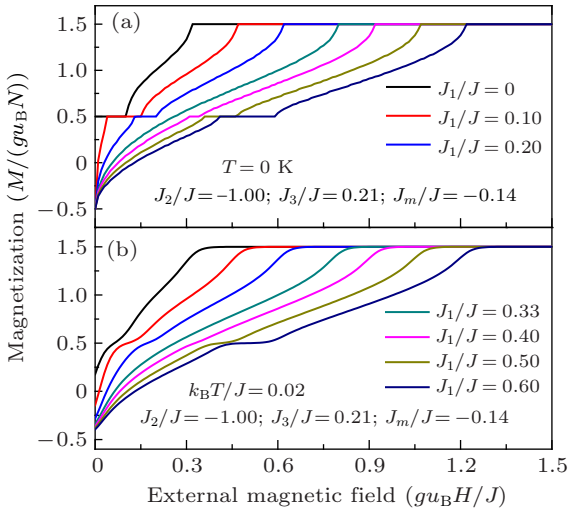


Fig. 8. The magnetization changes with the external magnetic field at (a) $T = 0$ K and (b) finite temperature $k_BT/J = 0.02$, under different antiferromagnetic exchange integrals J_1/J (0.0, 0.1, 0.2, 0.33, 0.4, 0.5, 0.6) (other parameters are set as $J_2/J = -1$, $J_3/J = 0.21$, $J_m/J = -0.14$).

It can be seen from Figs. 8 and 10 that the critical magnetic field intensities H_{CB}, H_{CE} and H_{CS} increase (all move to the right) with the increase of the reduced antiferromagnetic exchange integrals (J_1/J, J_3/J), and the region of spin-flop states widens. However, if only J_1/J is changed (see Figs. 8(a) and 9), the 1/3 magnetization plateau disappears when the $J_1/J = 0.33$ at 0 K. As can be seen from Figs. 7(b) and 9(b), thermal disorder energy k_BT accelerates the decrease and the increase of the width of the 1/3 magnetization plateau and the region of spin-flop states, respectively.

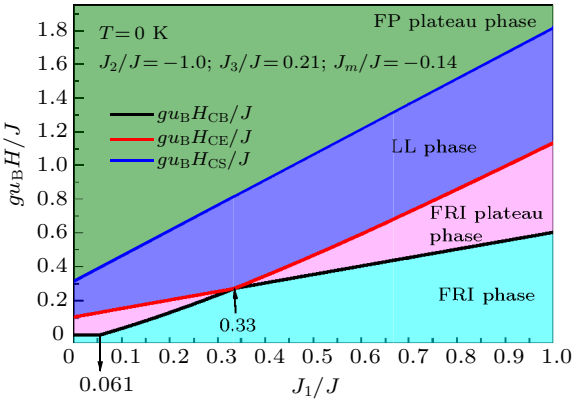


Fig. 9. The critical magnetic field intensities (H_{CB}, H_{CE} and H_{CS}) as a function of J_1 at $T = 0$ K (other parameters are set as $J_2/J = -1.0$, $J_3/J = 0.21$, $J_m/J = -0.14$).

As can be seen from Fig. 9, in a spin-1/2 alternating ferrimagnetic diamond chain at $T = 0$ K, when $J_2/J = -1.0$, $J_3/J = 0.21$, $J_m/J = -0.14$, and the antiferromagnetic exchange integral $J_1/J < 0.061$, as the antiferromagnetic exchange integral J_1 increases, the width of the 1/3 magnetization plateau of the system increases more and more. And with the increase of J_1, the saturation critical magnetic field intensity H_{CS} and H_{CE} increases linearly, and the increase in the amplitude and rate of H_{CS} is greater than that of H_{CE}, so the region of spin-flop states has expanded. This is because the critical magnetic field intensity H_{CB} does not change with J_1 in this range ($J_1/J < 0.061$). When $0.061 < J_1/J < 0.33$, as the antiferromagnetic exchange integral J_1 increases, the critical magnetic field intensity H_{CB} begins to increase linearly, and the rate of increase is greater than that of H_{CE}. As a result, the 1/3 magnetization plateau gradually decreases until it completely disappears near $J_1/J = 0.33$. When $J_1/J > 0.33$, the 1/3 magnetization plateau and the region of spin-flop states

gradually increase with the increase of J_1. Here, the 1/3 magnetization plateau disappears at the three-phase critical point of the FRI phase, the FRI plateau phase, and the LL phase. The critical antiferromagnetic exchange integral corresponding to this three-phase critical point is $J_1/J = 0.33$ (see Fig. 9).

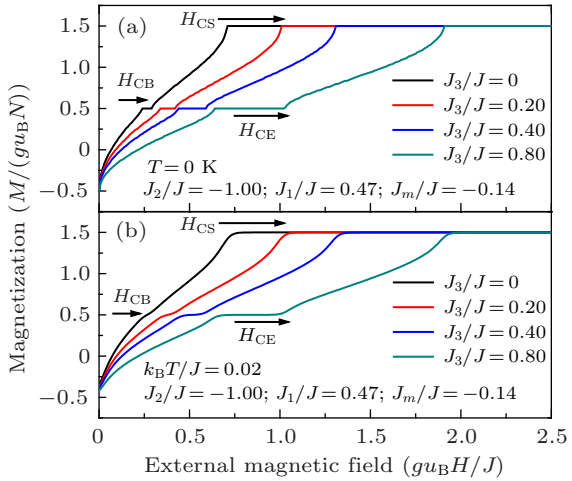


Fig. 10. The magnetization changes with the external magnetic field at (a) $T = 0$ K and (b) finite temperature $k_BT/J = 0.02$, under different anti-ferromagnetic exchange integrals J_3/J (0.0, 0.2, 0.4, 0.8) (other parameters are set as $J_2/J = 1$, $J_1/J = 0.47$, $J_m/J = 0.14$).

It can be seen from Figs. 11 and 12 that when the reduced exchange integral $J_1/J = 0.47$, $J_2/J = -1$, $J_3/J = 0.21$ is unchanged, at $T = 0$ K (see Figs. 11(a), 11(b) and 12), when $-J_m/J < 0.184$, the critical magnetic field intensity H_{CE} decreases (i.e., moves to the left) with the ferromagnetic exchange integral $-J_m/J$ increase. However, the critical magnetic field intensities H_{CB} and H_{CS} do not change, resulting in the width of 1/3 magnetization plateau gradually decreasing and the region of spin-flop states gradually expanding. When $-J_m/J = 0.184$, the 1/3 magnetization plateau disappears completely. When $0.336 > -J_m/J > 0.184$, the critical magnetic field intensity H_{CB} decreases (i.e., moves to the left), but the critical magnetic field intensities H_{CE} and H_{CS} do not change, resulting in the width of 1/3 magnetization plateau gradually increasing, and the region of spin-flop states are constant and independent of J_m. When $-J_m/J > 0.366$, the three critical magnetic field intensities H_{CB}, H_{CE} and H_{CS} are constant and independent of the ferromagnetic exchange integral J_m. Therefore, when $-J_m/J > 0.366$, the width of the 1/3 magnetization plateau and the width of the region of spin-flop states are constant and independent of J_m. Here, the 1/3 magnetization plateau disappears at the three-phase critical point of the FRI phase, the FRI plateau phase, and the LL phase. The critical ferromagnetic exchange integral corresponding to this three-phase critical point is $-J_m/J = 0.184$ (see Fig. 12).

When $-J_m/J = 0.184$, the 1/3 magnetization plateau completely disappears, and under the effect of thermal disorder energy k_BT outside the FP plateau region, this magnetization curve is separated from the magnetization curve in other cases ($J_m/J = 0.0$, -0.05, -0.1, -0.15, -0.25, -0.3, -0.35) at the finite temperature $k_BT/J = 0.01$ except for the FP plateau region (see Figs. 11(c) and 11(d)). This shows that there is a competition between magnetic order, which is caused by an external magnetic field in the system, and thermal disorder at finite temperatures.

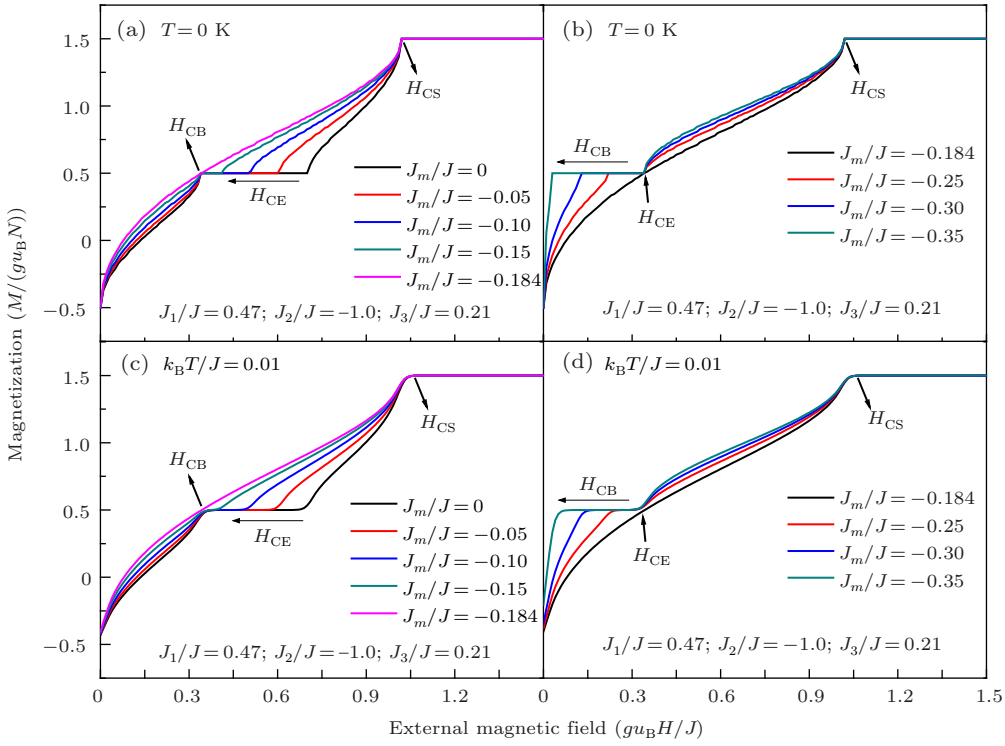


Fig. 11. The magnetization changes with the external magnetic field at (a), (b) $T = 0$ K and (c), (d) finite temperature $k_BT/J = 0.01$, under different ferromagnetic exchange integrals J_m/J (0.0, -0.05, -0.1, -0.15, -0.184, -0.25, -0.3, -0.35) (other parameters are set as $J_1/J = 0.47$, $J_2/J = -1.0$, $J_3/J = 0.21$).

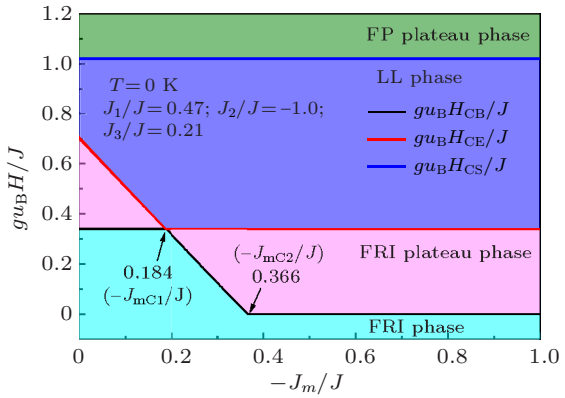


Fig. 12. The critical magnetic field intensities ($H_{\rm CB}$, $H_{\rm CE}$ and $H_{\rm CS}$) as a function of J_m/J at $T = 0$ K (other parameters are set as $J_1/J = 0.47$, $J_2/J = -1$, $J_3/J = 0.21$).

4. Conclusion

We have obtained the following conclusions by studying the magnetization and magnetic phase diagram of the spin-1/2 alternating ferrimagnetic diamond chain in external magnetic fields at finite temperatures.

(1) There are three critical magnetic field intensities $H_{\rm CB}$, $H_{\rm CE}$ and $H_{\rm CS}$ in the system. By analyzing the analytical solution of the elementary excitation spectra of the system under the external magnetic field at absolute zero, we find that there is the following correspondence between the elementary excitation spectra and the critical magnetic field intensities. $H_{\rm CB}$ and $H_{\rm CE}$ are respectively the external magnetic field intensities under which $\left[\hbar\omega_{3,k}(H_{\rm CB})\right]_{\rm min} = 0$ and $\left[\hbar\omega_{2,k}(H_{\rm CB})\right]_{\rm max} = 0$, while $H_{\rm CS}$ corresponds to $\left[\hbar\omega_{2,k}(H_{\rm CB})\right]_{\rm min} = 0$.

(2) The 1/3 magnetization plateau will inevitably disappear as long as the three-phase critical point exists in the magnetic phase diagram, which is intersected by the FRI phase, the FRI plateau phase, and the LL phase. However, the 1/3 magnetization plateau will not disappear without this three-phase critical point.

(3) The UP and the DN energy gap induce the appearance of the FP and the FRI plateau phase, respectively. Also, $\hbar\omega_{2,k}$ and $\hbar\omega_{3,k}$ can be positive or negative in the Brillouin zone, resulting in a gapless state in the system, then inducing the appearance of the LL and the FRI phase, respectively.

(4) The width of the 1/3 magnetization plateau is the largest at 0 K. As the temperature increases, $H_{\rm CB}$ gradually increases, while $H_{\rm CE}$ decreases, resulting in the width of 1/3 magnetization plateau gradually decreasing. Therefore, the appearance of the 1/3 magnetization plateau in the low-temperature region is the macroscopic expression of the quantum effect.

(5) The change of the ferromagnetic exchange energy $-J_2$ does not change $H_{\rm CB}$ and $H_{\rm CS}$. However, $H_{\rm CE}$ decreases with the increase of $-J_2$. As a result, the width of the 1/3 magnetization plateau decreases and the region of spin-flop states gets enlarged.

(6) There are two critical values ($-J_{\rm mC1}$ and $-J_{\rm mC2}$) for the ferromagnetic exchange integral $-J_m$. When $-J_m < -J_{\rm mC1}$, as $-J_m$ increases, $H_{\rm CE}$ decreases, but $H_{\rm CB}$ and $H_{\rm CS}$ remain unchanged, resulting in the width of the 1/3 magnetization plateau decreasing and the region of spin-flop states enlarged. When $-J_m = -J_{\rm mC1}$, the 1/3 magnetization plateau disappears completely. When $-J_{\rm mC2} > -J_m > -J_{\rm mC1}$, as $-J_m$ increases, $H_{\rm CB}$ decreases, but $H_{\rm CE}$ and $H_{\rm CS}$ remain unchanged, resulting in the width of the 1/3 magnetization plateau gradually increases, while the region of spin-flop states is unchanged. When $-J_m > -J_{\rm mC2}$, the three critical magnetic field intensities $H_{\rm CB}$, $H_{\rm CE}$ and $H_{\rm CS}$ are not related to $-J_m$.

(7) $H_{\rm CB}$, $H_{\rm CE}$, and $H_{\rm CS}$ increase with the antiferromagnetic exchange integral (J_1 or J_3). While the change of J_1 or J_3 can tune the 1/3 magnetization plateau, so that the width of the 1/3 magnetization plateau of the system changes from large to small until it disappears, and then increases. The above results indicated that the appearance of the 1/3 magnetization plateau is closely related to the magnetic ordered structure of the system.

References

[1] Shiomi D, Nishizawa M, Sato K, Takui T, Itoh K, Sakurai H, Izuoka A and Sugawara T 1997 *J. Phys. Chem. B* **101** 3342

[2] Kikuchi H, Fujii Y, Chiba M, Mitsudo S, Idehara T, Tonegawa T, Okamoto K, Sakai T, Kuwai T and Ohta H 2005 *Phys. Rev. Lett.* **94** 227201

[3] Yamaguchi T, Drechsler S L, Ohta Y and Nishimoto S 2020 *Phys. Rev. B* **101** 104407

[4] do Nascimento-Junior A M and Montenegro-Filho R R 2019 *Phys. Rev. B* **99** 064404

[5] Rule K C, Wolter A U B, Süllow S, Tennant D A, Brühl A, Köhler S, Wolf B, Lang M and Schreuer J 2008 *Phys. Rev. Lett.* **100** 117202

[6] Jeschke H, Opahle I, Kandpal H, Valentí R, Das H, Saha-Dasgupta T, Janson O, Rosner H, Brühl A, Wolf B, Lang M, Richter J, Hu S, Wang X, Peters R, Pruschke T and Honecker A 2011 *Phys. Rev. Lett.* **106** 217201

[7] Maisinger K, Schollwöck U, Brehmer S, Mikeska H J and Yamamoto S 1998 *Phys. Rev. B* **58** R5908

[8] Wang X, Zotos X, Karadamoglou J and Papanicolaou N 2000 *Phys. Rev. B* **61** 14303

[9] Schollwöck U 2005 *Rev. Mod. Phys.* **77** 259

[10] Cheng T M, Ma Y M, Ge C Y, Sun S S, Jia W Y, Li Q Y, Shi X F, Li L and Zhu L 2013 *J. Korean Phys. Soc.* **62** 104

[11] Fan H Y and Li C 2004 *Phys. Lett. A* **321** 75

[12] Fan H Y and Wu H 2005 *Mod. Phys. Lett. B* **19** 1361

[13] Batista C D and Ortiz G 2001 *Phys. Rev. Lett.* **86** 1082

[14] Verkholyak T, Strečka J, Jaščur M and Richter J 2011 *Eur. Phys. J. B* **80** 433

[15] da Silva W M and Montenegro-Filho R R 2017 *Phys. Rev. B* **96** 214419

[16] Zapf V, Jaime M and Batista C D 2014 *Rev. Mod. Phys.* **86** 563

[17] Giamarchi T, Rüegg C and Tchernyshyov O 2008 *Nat. Phys.* **4** 198

[18] Oshikawa M, Yamanaka M and Affleck I 1997 *Phys. Rev. Lett.* **78** 1984

[19] Courant R and Hilbert D 1968 *Methoden der Mathematischen Physik I*, (Springer-Verlag Berlin·Heidelberg·New York) p. 36

[20] Wang Z X and Guo D R 2010 *Introduction to special functions* (first edition) (Beijing: Peking University Press) p. 480 (in Chinese)